International Journal of Engineering Science 134 (2019) 66–76

Contents lists available at ScienceDirect

International Journal of Engineering Science

journal homepage: www.elsevier.com/locate/ijengsci

On a combined thermal/mechanical performance of a foam-filled sandwich panels

Yury Solyaev[a,b,*], Sergey Lurie[a,b], Alla Koshurina[b], Vasiliy Dobryanskiy[c], Mark Kachanov[b,d]

[a] Institute of Applied Mechanics of Russian Academy of Sciences, Moscow, Russia
[b] Nyzhny Novgorod State Technical University named after R. E. Alekseev, Nyzhny Novgorod, Russia
[c] Moscow Aviation Institute, Moscow, Russia
[d] Department of Mechanical Engineering, Tufts University, Medford, MA 02155, USA

ARTICLE INFO

Article history:
Received 28 October 2018
Accepted 29 October 2018

Keywords:
Sandwich panel
Corrugated core
Filling foam
Optimization
Thermal insulation
Effective winkler moduli

ABSTRACT

The structure of a foam-filled corrugated core sandwich panel is optimized. Failure modes under consideration are the overall and local instability of the panel. Models of plates resting on an elastic foundation are used to take into account the foam's reinforcement effect. Additional constraint related to the effective thermal conductivity of the panel is incorporated.

1. Introduction

Sandwich panels attract an increasing attention due to being lightweight and, at the same time, meeting the requirements of strength, stiffness, energy absorption, thermal resistance etc. – provided their design is optimized appropriately (see Birman & Kardomatea, 2018; Vescovini, D'Ottavio, Dozio, & Polit, 2018; Vinson, 2005). Among sandwich structures, the corrugated-core panels usually have an optimal combination of the load-bearing capacity and thermal resistance. They have lower thermal conductivity than structures with honeycomb cores, and structural performance, stiffness, and strength are higher than the foam-core panels (Bitzer, 2012; Njuguna, 2016). These features make the corrugated cores the ones of choice in multi-functional applications such as thermally insulated load-bearing structural elements (Bapanapalli et al., 2006), actively cooled aircraft skins (Xie, Wang, Ji, & Sunden, 2016) and heat exchangers (Lu, Valdevit, & Evans, 2005).

In the present study, we consider an optimization problem for panels used as structural elements of the rescue vehicles operating in extreme environmental conditions (such as arctic oil platforms). The possibility to satisfy a combination of the strength, stiffness, and thermal insulation/protection requirements was discussed in recent works of Lurie, Solyaev, Volkov-Bogorodskiy, Bouznik, and Koshurina (2017); Lurie et al. (2018) and Buznik et al. (2016). It was found that the limit state of considered panels is defined by local buckling of the panel elements under mechanical loading provided external cooling is used (that prevents overheating and thermally induced buckling during operating under the burning oil conditions).

* Corresponding author at: Institute of Applied Mechanics of Russian Academy of Sciences, Moscow, Russia.
E-mail address: yos@iam.ras.ru (Y. Solyaev).

https://doi.org/10.1016/j.ijengsci.2018.10.010
0020-7225/

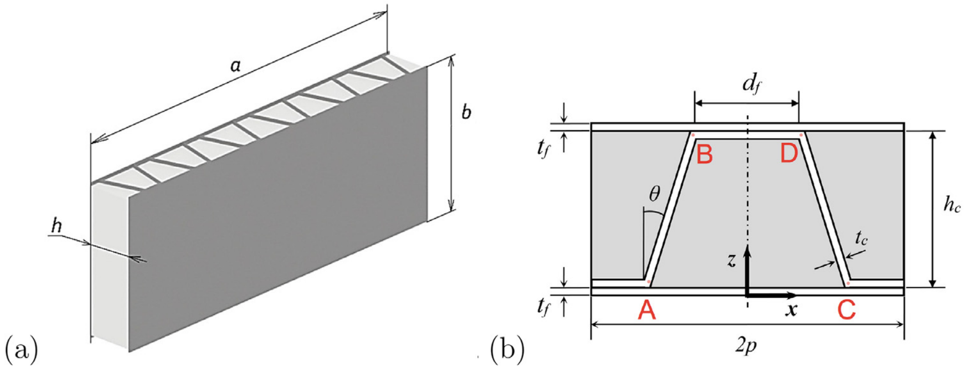

Fig. 1. Corrugated core sandwich panel (a) and its unit cell (b).

The present work focuses, to large extent, on the effects produced by foam. An optimization problem, with regard to the mentioned limit states, is considered.

Foam-filled sandwich panels with web cores (with vertical plate elements (struts) regularly placed inside the foam core) have been considered in several works. In-plane compression of such panels was considered in the work of Aimmanee and Vinson (2002), where closed form analytical solutions were obtained for weight minimization. Foam reinforcement effect was taken into account by considering models of plates (face sheets, web elements) resting on an elastic foundation. Analysis of panels under shear loading was performed by Briscoe, Mantell, and Davidson (2010) using the Pasternak foundation model. Design procedure for the roof panels with foam-filled web-core was developed by Briscoe, Mantell, Davidson, and Okazaki (2011) with the thermal resistivity constraints taken into account. Panels with lattice cores were investigated experimentally and analytically by Wang, Liu, Wan, Fang, and Hui (2014).

As far as panels with the foam-filled corrugated cores are concerned, their stability under transverse shear was considered by Bin et al. (2015), with further work on their optimization done by Han et al. (2015). The general optimization procedure for the foam-filled corrugated core sandwiches have not been considered, to our knowledge. One of the difficulties lies in the non-uniform thickness of the foam (Fig. 1) that leads to variable stiffness of the elastic foundation that should be taken into account in the local buckling models. Bin et al. (2015) proposed to evaluate the local stability of the inclined web elements under transverse shear by taking into account periodic and symmetric structure of the panel's unit cells. The value of Winkler modulus was estimated by modeling the foam by a system of springs oriented in the vertical and horizontal directions. However, for the face plate elements such simplifications cannot be used. The present work utilizes results for plate elements resting on a variable elastic foundation. The effective Winkler moduli of the foundation are introduced based on solution for the buckling deflection. Failure/thermal performance maps are constructed.

2. Model

We develop analytical models for the panel mechanical and thermal performance; we disregard thermally-induced buckling assuming that an external cooling system (activated in the case of fire) is used (Lurie et al., 2018).

2.1. Structural parameters of the panel

We consider a sandwich panel with corrugated core shown in Fig. 1 where notations are as follows. The face thickness is t_f, the web thickness is t_c and the core depth is h_c, The distance between the web elements is d_f, the corrugation pitch is $2p$, and the angle between the web and the vertical direction is θ. The total panel thickness is $h = h_c + 2t_f$. Length of the inclined core plate element AB will be denoted as $l = h_c/\cos\theta$. Length of the face plate element AC is $d = 2p - d_f$. The panel length is a and its width is b. The number of the core pitches across the panel length is $N = a/(2p)$. Internal panel surface is located at $z = 0$ and the external one at $z = h$ in the coordinate system shown in Fig. 1a. Material of the load bearing elements (faces and core) is the glass fiber reinforced plastic with symmetric quasi-isotropic lay-up. Thermal-insulating foam material fills the free space inside the panel.

2.2. Effective properties of the panel and of the core

The average mass density of the panel $\rho = (2\rho_f A_f + \rho_c A_c + \rho_p A_p)/A$, where indexes f, c and p correspond to the face plate, core and foam materials; $A = 2ph$ is the total area of the unit cell's cross section; $A_f = 2pt_f$, $A_c = 2t_c(d_f + l)$, $A_p = A - 2A_f - A_c$ are the areas of the corresponding parts of the cross section. Mass per unit area of the panel, which will be minimized in the optimal design procedure in the following, can be evaluated as $m = h\rho$.

The effective thermal conductivity of the panel in thickness direction is evaluated by the law of mixtures, as done in a number of works on the subject (Bapanapalli et al., 2006; Martinez, Sankar, Haftka, Bapanapalli, & Blosser, 2007) and given by:

$$k = \frac{2k_f A_f + k_c A_c + k_p A_p}{A} \tag{1}$$

Sufficient accuracy of the relation (1) in the context of the considered sandwich has been shown by Bapanapalli et al. (2006), Martinez et al. (2007) and Lurie et al. (2017).

Bending stiffnesses of the panel D_{ij} is relevant for stability under compression. For the considered orthotropic structure,

$$D_{ij} \approx Q_{ij}\frac{h_c^2 t_f}{2} + Q_{ij}^*\frac{h_c^3}{12} \tag{2}$$

where the Voigt's notation is used; $Q_{11} = Q_{22} = E/(1-\nu^2)$, $Q_{12} = \nu Q_{11}$, $Q_{66} = G$ are the stiffness constants of the face plates; $Q_{22}^* = EA_c/(2ph_c(1-\nu^2))$, $Q_{11}^* = Q_{12}^* = Q_{66} = 0$ are the effective stiffnesses constants of the corrugated core, which provide a reinforcement effect only in the y-axis direction (Vinson, 1999); E, G, ν are the Young's modulus, shear modulus and Poisson's ratio of the faces and core material. The foam's reinforcement effect on bending stiffness of the panel is neglected.

For evaluation of the panel's local stability we use models of plates resting on an elastic foundation, with Winkler foundation modulus related to the foam's elastic properties and geometric parameters of the panel. As shown by Bin et al. (2015), for the inclined elements of the corrugated core (AB in Fig. 1b) the surrounding foam can be treated as a superposition of two types of elastic foundations having constant moduli and oriented vertically and horizontally. Simplified evaluations for these moduli were performed based on classical approach (see Kerr, 1985). The overall foundation modulus has the form:

$$\Lambda = \Lambda_h \cos\theta + \Lambda_v \sin\theta, \tag{3}$$

where $\Lambda_h = \bar{E}_p/p$, $\Lambda_v = \bar{E}_p/h_c$ are the foundation moduli in the horizontal and vertical directions, respectively; $\bar{E}_p = E_p/(1-\nu_p^2)$ is the elastic stiffness constant of the foam; E_p and ν_p are the Young's modulus and Poisson's ratio of the foam.

Winkler modulus for the face plates elements (AC in Fig. 1b) is different for the three regions across the length of an element. For the middle region, we assume that the opposite face element AD (stacking with web core horizontal plate) remains undeformed while the element AC buckles. Thus, the Winkler modulus of the middle region is evaluated as:

$$\Lambda_0 = \frac{\bar{E}_p}{h_c - t_c}, \quad x \in [-d_f/2, d_f/2] \tag{4}$$

As far as the edge regions are concerned, we assume, that, in the first approximation, that the reinforcment effect of the inclined web element can be neglected. Thus, due to the symmetry of the panel geometry we have:

$$\Lambda_1 = \frac{2\bar{E}_p}{h_c}, \quad x \in [-d/2, -d_f/2] \cup [d_f/2, d/2] \tag{5}$$

2.3. Failure modes

We consider a panel loaded by in-plane compression stress, with resultant per unit width $N_{\max}$ – the loading condition relevant for operating conditions of the vehicle. The maximal value of the compression resultant $N_{\max}$ corresponds to the overturning of the vehicle.

For estimation of the normal stresses in panel elements we will take into account that the axial loading $N_{\max}$ is resisted by the corrugated core elements and face plates. The influence of the foam can be neglected due to its low stiffness. Assuming uniform boundary conditions for the tractions, we have the following normal stress in the face plates and core elements:

$$\sigma_{max} = \frac{2pN_{max}}{A_f + A_c} \tag{6}$$

Note, that safety factor for the face and core materials failure under compression usually used in design is $K_y = \sigma_u/\sigma_{\max}$, where σ_u is the compression strength of the panel material. Evaluation of the foam strength will be out of consideration because under the in-plane loading the deformations of the core will be relatively small, and the limit state of the panel will be defined by the failure of the faces and of the core web elements.

2.3.1. Panel overall stability

First assessment for the panel overall stability is obtained based on the classical theory of plates following Vasiliev and Morozov (2013); Vinson (1999). Critical load per unit width and corresponding safety factor are defined by relations:

$$N_{cr} = \frac{\pi^2\sqrt{D_{11}D_{22}}}{a^2}\left(\sqrt{\frac{D_{11}}{D_{22}}}\left(\frac{m}{c}\right)^2 + \frac{2(D_{12}+2D_{66})}{\sqrt{D_{11}D_{22}}} + \sqrt{\frac{D_{22}}{D_{11}}}\left(\frac{c}{m}\right)^2\right), \tag{7}$$

$$K_{cr} = \frac{N_{cr}}{N_{max}},$$

where $c = a/b$ – is the aspect ratio of panel, m – is the number of half waves, appearing in buckling in the direction perpendicular to the load and determined from inequalities: $m(m-1) < c^2\sqrt{D_{22}/D_{11}} < m(m+1)$ (Vasiliev & Morozov, 2013).

2.3.2. Web plate buckling

Critical compression stress for the buckling of the corrugated core elements can be evaluated based on the known solution for the thin plate on an elastic foundation with simply supported edges, see, for example, Yu and Wang (2008). The critical stress is given by:

$$\sigma_c = \frac{\pi^2 D_c}{l^2 t_c}\left(\frac{n\,l}{b} + \frac{b}{n\,l}\right)^2 + \frac{\Lambda}{t_c}\left(\frac{b}{n\pi}\right)^2, \tag{8}$$

where $D_c = E\,t_c^3/(12(1-\nu^2))$ is the bending stiffness of the core plate element; n is the number of half waves in the y-axis direction over which the plate buckles (in analytical solution the value of n should be chosen to provide the minimum value of σ_c); Λ is the Winkler modulus of the elastic foundation (3).

Safety factor for the core's elements stability under compression defined as $K_c = \sigma_c/\sigma_{\max}$.

2.3.3. Face plate buckling

The problem of face plate buckling is more complex than the one for the web elements, because the same simple definitions for the constant foundation modulus cannot be used. A simplified approach proposed here is to divide the length of the face plate element into three regions with constant values of the foundation moduli: Λ_0 in the middle region and Λ_1 around the edges under the inclined core elements. Solution is given in Appendix. Critical buckling stress under compression is given by:

$$\begin{aligned}
\sigma_f &= \frac{\sigma_1 + \sigma_3 - \sqrt{4\,\sigma_{1\text{-}3}^2 + (\sigma_1 - \sigma_3)^2}}{2},\\
\sigma_1 &= \frac{\pi^2 D_f}{d^2 t_f}\left(\frac{n\,d}{b} + \frac{b}{n\,d}\right)^2 + \frac{\Lambda_1^*}{t_f}\left(\frac{b}{n\pi}\right)^2,\\
\sigma_3 &= \frac{\pi^2 D_f}{d^2 t_f}\left(\frac{n\,d}{b} + \frac{9\,b}{n\,d}\right)^2 + \frac{\Lambda_3^*}{t_f}\left(\frac{b}{n\pi}\right)^2,\\
\sigma_{1\text{-}3} &= \frac{\Lambda_{13}^*}{t_f}\left(\frac{b}{n\pi}\right)^2
\end{aligned} \tag{9}$$

where $D_f = E\,t_f^3/(12(1-\nu^2))$ is the bending stiffness of the face plate element; number of half waves n should be chosen to minimize σ_f; the effective Winkler moduli Λ_1^*, Λ_3^*, Λ_{13}^* of the variable elastic foundation depend on core stiffnesses Λ_0, Λ_1 and geometric ratio $\alpha = d_f/d$ as follows (see Appendix):

$$\begin{aligned}
\Lambda_1^* &= \Lambda_1 + \alpha(\Lambda_0 - \Lambda_1)\left(1 - \frac{\sin(\pi\alpha)}{\pi\alpha}\right),\\
\Lambda_3^* &= \Lambda_1 + \alpha(\Lambda_0 - \Lambda_1)\left(1 - \frac{\sin(3\pi\alpha)}{3\pi\alpha}\right),\\
\Lambda_{13}^* &= (\Lambda_0 - \Lambda_1)\left(\frac{\sin(\pi\alpha)}{\pi\alpha} - \frac{\sin(2\pi\alpha)}{2\pi\alpha}\right),
\end{aligned} \tag{10}$$

Safety factor for the face plate buckling is introduced as $K_f = \sigma_f/\sigma_{\max}$.

2.4. Thermal performance

Requirements for thermal insulation behavior of the panel will be stated in terms of the effective thermal conductivity (1). Maximum allowable coefficient of thermal conductivity of the panel, that is implied by the operating requirements is $k_{\max}$, with the safety factor for the thermal performance $K_T = k_{\max}/k$.

3. Statement of the optimization problem

We consider an optimization problem to determine the geometric parameters $\{t_f, t_c, h_c, d_f, N\}$ that provide a minimum mass per unit area of the panel $m = \rho h$. All other geometric parameters of the panel can be estimated if its dimensions a and b are given, namely, the corrugation ptich is estimated as $2p = a/N$. The constraints of the problem are prescribed in terms of safety factors defined above. The following statement of the problem is given, that define, a non-linear global

Table 1
Material properties.

Material	Density, kg/m^3 kg/m^3	Thermal Conductivity, W/(mK)	Young's modulus, MPa	Poisson's ratio	Compression strength, MPa
GFRP	1800	1	22,000	0.25	380
Foam	30	0.05	0.5	0.4	-
Rockwool	25	0.03	-	-	-

Table 2
Ranges of the design variables.

Parameter		Minimum value	Maximum value
t_f	mm	1	4
t_c	mm	0.5	2
h_c	mm	10	300
d_f	mm	0 (truss core)	p (web core)
N	-	8	12

optimization problem with inequalities constraints:

$$\begin{cases} \min: & m(t_f, t_c, h_c, d_f, N) \\ s.t.: & K_y > 1,\ K_{cr} > 1,\ K_T > 1, \\ & K_c > 1,\ K_f > 1 \end{cases} \tag{11}$$

where the first row of the constraints represents safety factors for the structural material failure, overall stability and thermal insulation and the second row relates to the local buckling safety factors.

Additionally, one should take into account certain geometric restrictions (e.g. $0 \le \alpha \le 1$) and manufacturing constraints. Solution of (11) can be found by using standard non-linear global optimization methods that can be applied to the problems with inequalities constraints. Namely, we used the "simulated annealing" and direct random search methods implemented in the Wolfram Mathematica system with *machine precision* setting.

4. Results and discussion

4.1. Initial data

In our calculations we will find an optimal geometry of unit cells and failure mechanisms map for sandwich panel with dimensions $a = 1200$ mm and $b = 500$ mm. Materials properties are given in Table 1. High temperature polyamide foam is used as the filler, because the safety norms require the maximum continuous service temperature of the foam not smaller than 300 °C. Comparison is given with fibrous insulation filler made of rockwool, which has lower density and thermal conductivity and does not provide any significant reinforcement effect.

Two cases of the prescribed compression and shear forces per unit of the panel width are considered. In the first case (I): $N_y = 0.5 \cdot 10^4$ N/m, and in the second one (II): $N_y = 5 \cdot 10^4$ N/m. The maximum allowable coefficient of thermal conductivity of the panel is $k_{\max} = 0.1$ W/(mK). The ranges of design variables are presented in Table 2 that take into account technological limitations.

4.2. Local buckling of face plates

We present results of evaluation of the face plate local buckling that were obtained based on the solution (9). We consider a face plates of different aspect ratio b/d and different parameters of the foundation that are defined by the foam properties and geometry of the web core. The influence of core stiffness and geometry on the buckling stress of the face plate element is presented in Figs. 2 and 3. It is shown that the foundation is always increase the critical stress, especially for the short plates. The presence of even soft foam increases the critical buckling stress with factor of two and more (see Fig. 2). The core geometry also significantly influences the critical load. Namely, for the cores, with geometry close to truss of small thickness (i.e. with low d_f/d ratio and small h_c), the critical stress increases (see Fig. 3). This effect is explained by the decrease of the relative area of the soft middle region in the elastic foundation and by the inverse dependence of the Winkler moduli on the foundation thickness.

4.3. Solution of the optimization problem

Solution of the thermo-structural optimization problem (11) can be obtained by utilizing the Wolfram Mathematica software using "simulated annealing" and direct random search methods, with predefined ranges of geometric parameters and

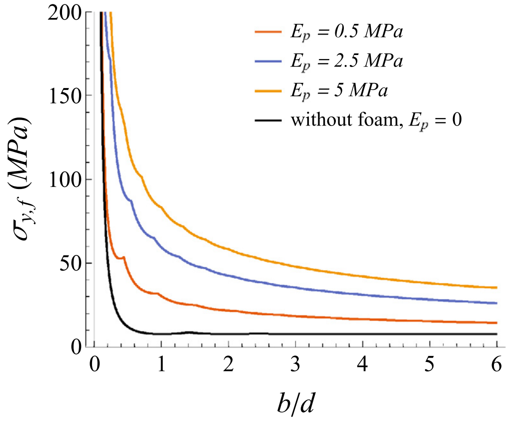

Fig. 2. Dependence of the face plate buckling compression stress on the aspect ratio b/d for different Young's modulus of the foam. Geometric parameters: $d = 100$ mm, $h_c/b = 0.1$, $\alpha = 0.5$, $t_f = t_c = 1$ mm.

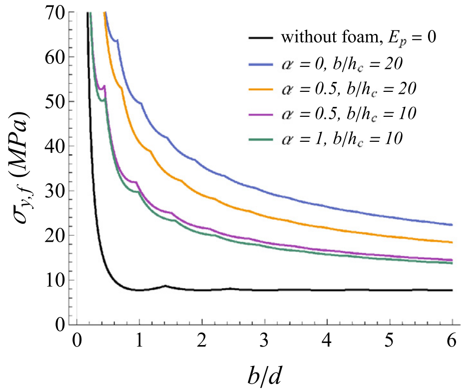

Fig. 3. Dependence of the face plate buckling compression stress on the aspect ratio b/d ratio for different ratios b/h_c and $\alpha = d_f/d$. Case $\alpha = 0$ and $\alpha = 1$ correspond to truss and web cores, respectively. Geometric and elastic parameters: $d = 100$ mm, $t_f = t_c = 1$ mm, $E_p = .5$ MPa.

Table 3
Optimization results.

Parameters and safety factors		Foam		Rockwool	
		I	II	I	II
t_f	mm	1	1	2.7	-
t_c	mm	0.5	1	1.9	-
h_c	mm	47	70	120	-
d_f	mm	0	56	0	-
N	mm	8	9	8	-
α	–	0	0.75	0	-
θ	deg	57	8	31	-
h	mm	49	72	125.4	-
m	kg/m^2	6.1	8.9	19.2	-
K_y	–	121	21	483	-
K_{cr}	–	181	44	3380	-
K_T	–	1	1	1	-
$K_{y,\,c}$	–	2.9	1	1	-
$K_{y,\,f}$	–	4	1	1	-

for the two loading levels. Obtained results are presented in Table 3. Both optimization methods provide the same solutions. The found optimal geometry of the unit cells for the panels with foam and fibrous insulation are compared in the Fig. 4. Note that a panel with fibrous insulation cannot be optimized for a higher loading level II. Solution of the optimization problem (11) does not exist in this case because the structural constraints related with failure and local buckling of the panel elements can not be fullfilled.

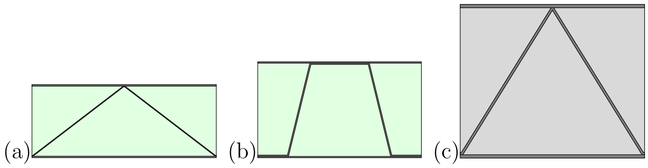

Fig. 4. Optimized geometry of the panel's unit cells; (a) – foam insulation, loading level I, (b) – foam insulation, loading level II, (c) – fibrous insulation, loading level I.

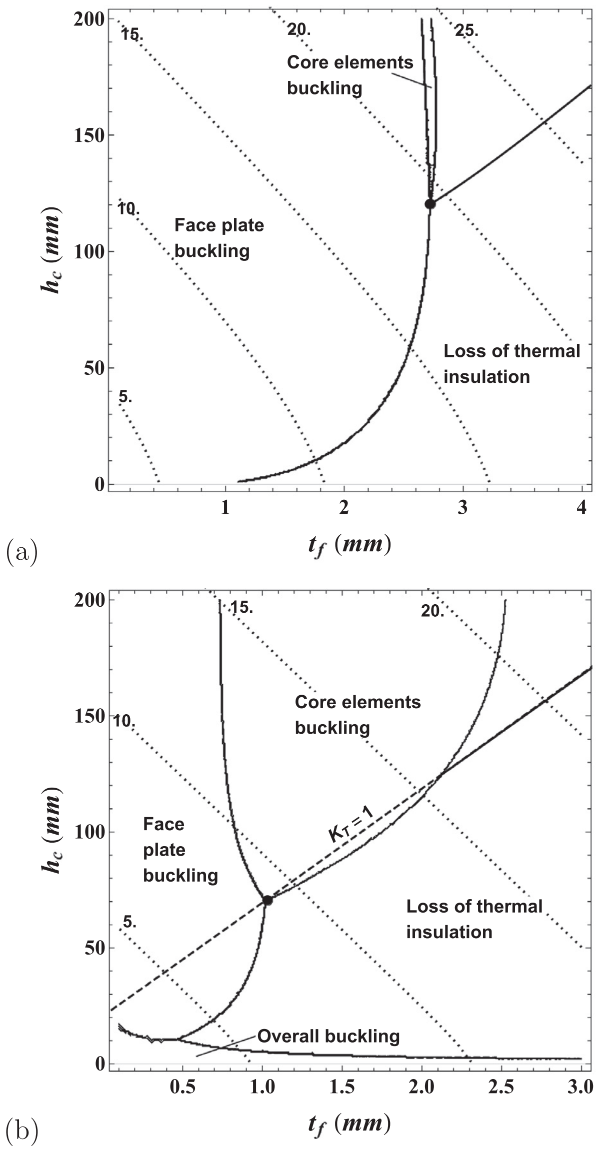

Fig. 5. Failure mechanism/thermal performance maps, (a): panel with fibrous filler, (b): panel with foam filler. Mass per unit area of the panel (m, kg/m^2) is shown by thin dotted lines and labels. Solutions of the optimization problems are shown by black dots.

From Table 3 and Fig. 4 one can see that the foam-filled truss-core panels ($\alpha \approx 0$) demonstrate the best thermal insulation performance and the optimized unit cells for the low loading level (I) have the triangular core (Fig. 4a). The limit state of these panels is defined by the thermal insulation requirement only, while the structural restrictions are fulfilled with sufficiently high safety factors. Thus, for the low loading levels considered foam-filled panels can be optimized based on the single criterium for the effective thermal conductivity (1) assuming $\alpha = 0$.

At high loads, truss core is not an optimal choice and the corrugated cores with $\alpha > 0$ are preferable for the loading level II (Fig. 4b). Optimal width of the unit cells reduces and thickness of the panel elements increases to provide stiffness and strength. Total thickness of the panels also increases, to provide an insulation level, because the presence of thick load-bearing elements leads to increase of the effective thermal conductivity of the panel. The same effect arises in a panel with fibrous insulation, which total thickness is very high because its elements are quite thick (Fig. 4c). Triangular core in this panel ensures additional decrease of thermal conductivity: in this case the inclined elements of the core are the longest and their impact on the effective conductivity reduces.

The considered foam filler allows one to reduce the mass per unit area by the factor of three in comparison with fibrous insulation under similar load. Additionally, the load-bearing capacity of the foam-filled panels can be increased by the factor of ten and more (loading level II) without loss of the insulation properties, if operating requirements allow an increase of the faces and core elements thickness with corresponding increase of the panel mass. Optimal variant of geometry ensuring the desirable specific strength and insulation level can be found by using the proposed model.

Note that foam-filled panels are more "balanced" with respect to different failure modes, in the sense that differences between different safety factors are smaller than in the case of panels with fibrous insulation (see Table 3).

4.4. Failure mechanism/thermal performance maps

Finally, we study the effect of filler on failure mechanisms (Fig. 5). The presented maps also indicate limits for the maximum thermal conductivity of the panel and the values of panel mass per unit area. The map for the foam-filled panel is given for the loading level II, and for the panel with fibrous insulation – for the level I. These levels correspond to limit states of the panels under high loading level close to their maximum load bearing capacity. Optimal values of t_c, d_f and N from Table 3 are used in these plots. It is seen that, for the sandwiches with soft fibrous filler the limit state is primarily defined by the local buckling of face plate and by the thermal insulation requirements (Fig. 5a). Core elements in these panels are rather thick and the area of their local buckling is very small and corresponds to high values of core thickness. For a foam-filled panel, relatively larger areas of different limit states are seen in the map (Fig. 5b). The optimization solution lies at intersection of three limit states of the panel – the ones determined by local buckling K_c, K_f, and thermal insulation K_T. Overall buckling area is also seen on this map and it is realized for rather thin panels that do not satisfy the thermal insulation requirements. Solutions of the optimization problem (11) are shown by black dots in Fig. 5. They define the minimum values of the geometric parameters that ensure satisfaction of all the thermal and mechanical restrictions and minimize the mass of the panel.

5. Conclusions

A general procedure for optimization of a foam-filled corrugated core sandwich panel under the in-plane compression combined with thermal load is outlined. It comprises an approximate solution for stability of plate elements under compression taking into account reinforcement effects of the filling foam. The effective Winkler moduli are introduced to describe the dependence of the elastic foundation stiffness on parameters of the foam. The considered optimization problem that covers a combination of the mechanical and thermal properties is highly non-linear. At low levels of mechanical loads the problem simplifies significantly.

Acknowledgements

This work was supported by grant 14.Z50.31.0036 awarded by Ministry of Science and Higher Education of the Russian Federation to R. E. Alexeev Nizhny Novgorod Technical University.

Appendix

Consider a face plate element of length b and width d resting on the Winkler elastic foundation of variable stiffness. Simply supported boundary conditions are assumed, to obtain the lower bound for the buckling load. For the prescribed uniform compression stress σ_f in the y-axis direction, the equation governing buckling deflection w is given by :

$$D_f \nabla^4 w + \sigma_f t_f w_{,yy} + \Lambda(x) w = 0, \quad x \in [-d/2, d/2], \quad y \in [0, b] \tag{12}$$

where $D_f = E t_f^3/(12(1-\nu^2))$ is bending stiffness of face plate element and Winkler modulus is a piecewise constant function:

$$\Lambda(x) = \begin{cases} \Lambda_1, & x \in [-d/2, -d_f/2] \\ \Lambda_0, & x \in [-d_f/2, d_f/2] \\ \Lambda_1, & x \in [d_f/2, d/2] \end{cases} \tag{13}$$

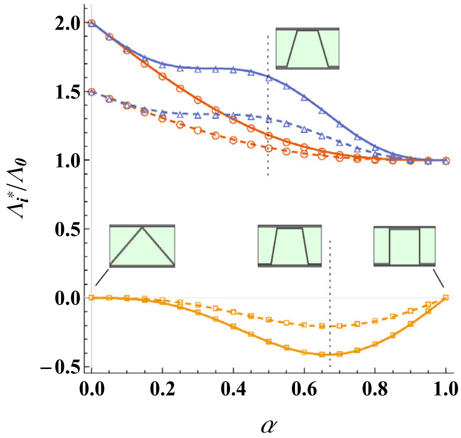

Fig. 6. Dependence of the normalized effective Winkler moduli Λ_1^* (circles), Λ_3^* (triangles) and Λ_{13}^* (squares) on the core geometric parameter $\alpha = d_f/d$. Solid lines: $\Lambda_1/\Lambda_0 = 2$, dashed lines: $\Lambda_1/\Lambda_0 = 1.5$.

The following representation for the deflection function that consists of only first and third harmonics in the x-axis direction is sought:

$$w(x, y) = \sum_{n=1}^{\infty}\left(A_n \cos\frac{\pi x}{d} + B_n \cos\frac{3\pi x}{d}\right)\sin\frac{n\pi y}{b} \tag{14}$$

so that strain energy of the buckled plate can be expressed as (Timoshenko & Gere, 1961):

$$\begin{aligned} U &= \frac{1}{2}\int_0^b \int_{-d/2}^{d/2} \left(D_f (w_{,xx} + w_{,yy})^2 + 2(1-\nu)(w_{,xx}w_{,yy} - w_{,xy}^2)\right)dxdy \\ &= \frac{D_f b d \pi^4}{8}\sum_{n=1}^{\infty}\left(A_n^2\left(\frac{1}{d^2}+\frac{n^2}{b^2}\right)^2 + B_n^2\left(\frac{9}{d^2}+\frac{n^2}{b^2}\right)^2\right) \end{aligned} \tag{15}$$

The work done by the external forces is:

$$\begin{aligned} V &= -\frac{1}{2}\int_0^b \int_{-d/2}^{d/2} \left(\sigma_f t_f w_{,y}^2 - \Lambda(x) w^2\right)dxdy \\ &-\frac{\sigma_f t_f d\,\pi^2}{8\,b}\sum_{n=1}^{\infty}(A_n^2 + B_n^2)n^2 \\ &+\frac{bd}{8}\sum_{n=1}^{\infty}\left(A_n^2\,\Lambda_1^* + 2A_nB_n\,\Lambda_{13}^* + B_n^2\,\Lambda_3^*\right), \end{aligned} \tag{16}$$

where the effective Winkler moduli Λ_1^*, Λ_3^*, Λ_{13}^* is found after integration of the piecewise function (13) as:

$$\begin{aligned} \Lambda_1^* &= \Lambda_1 + \alpha(\Lambda_0 - \Lambda_1)\left(1 - \frac{\sin(\pi\alpha)}{\pi\alpha}\right), \\ \Lambda_3^* &= \Lambda_1 + \alpha(\Lambda_0 - \Lambda_1)\left(1 - \frac{\sin(3\pi\alpha)}{3\pi\alpha}\right), \\ \Lambda_{13}^* &= (\Lambda_0 - \Lambda_1)\left(\frac{\sin(\pi\alpha)}{\pi\alpha} - \frac{\sin(2\pi\alpha)}{2\pi\alpha}\right), \end{aligned} \tag{17}$$

where $\alpha = d_f/d$ is the ratio defining the core geometry. The dependence of the effective Winkler moduli on α is presented in the Fig. 6. Note that for the web core sandwich panel ($\alpha = 1$) the effective Winkler moduli take minimal values: $\Lambda_1^* = \Lambda_3^* = \Lambda_0$ and $\Lambda_{13}^* = 0$. For the panels with truss cores (triangular corrugation with $\alpha = 0$), $\Lambda_1^* = \Lambda_3^* = \Lambda_1$ and, also, $\Lambda_{13}^* = 0$. For corrugated cores, the Winkler modulus Λ_3^* that is related to the third harmonics is larger than modulus Λ_1^* related to the first one, whereas modulus Λ_{13}^* has negative sign and defines coupling between these harmonics.

Using the variational approach, the first variation of the total potential energy is zero when the plate is in equilibrium:

$$\delta\Pi = \delta U + \delta V = 0, \quad i.e. \quad \frac{\partial\Pi}{\partial A_n} = 0, \quad \frac{\partial\Pi}{\partial B_n} = 0 \tag{18}$$

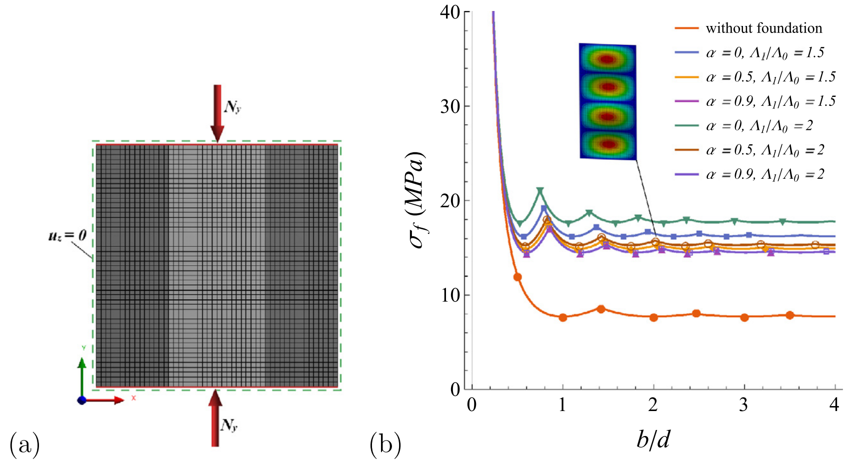

Fig. 7. Finite element validation of analytical solution for the critical stress σ_f of the plate resting on variable elastic foundation, $d = 100$ mm, $t_f = 1$ mm, $\Lambda_0 = 0.0125$ N/mm^3, a: finite element model, b: comparison between analytical (lines) and numerical (points) solutions.

Substituting (15) and (16) into (18) yields the following system of homogeneous equations:

$$\left(D_f\pi^4\left(\frac{1}{d^2}+\frac{n^2}{b^2}\right)^2-\frac{\sigma_f t_f n^2\pi^2}{b^2}+\Lambda_1^*\right)A_n+\Lambda_{13}^*B_n=0$$
$$\left(D_f\pi^4\left(\frac{9}{d^2}+\frac{n^2}{b^2}\right)^2-\frac{\sigma_f t_f n^2\pi^2}{b^2}+\Lambda_3^*\right)B_n+\Lambda_{13}^*A_n=0 \tag{19}$$

that can be rewritten as:

$$\left(\sigma_1-\sigma_f\right)A_n+\sigma_{1\text{-}3}B_n=0$$
$$\sigma_{1\text{-}3}A_n+\left(\sigma_3-\sigma_f\right)B_n=0 \tag{20}$$

where we introduce notations:

$$\sigma_1=\frac{\pi^2D_f}{d^2t_f}\left(\frac{n\,d}{b}+\frac{b}{n\,d}\right)^2+\frac{\Lambda_1^*}{t_f}\left(\frac{b}{n\pi}\right)^2,$$
$$\sigma_3=\frac{\pi^2D_f}{d^2t_f}\left(\frac{n\,d}{b}+\frac{9\,b}{n\,d}\right)^2+\frac{\Lambda_3^*}{t_f}\left(\frac{b}{n\pi}\right)^2,$$
$$\sigma_{1\text{-}3}=\frac{\Lambda_{13}^*}{t_f}\left(\frac{b}{n\pi}\right)^2 \tag{21}$$

The minimum value of σ_f that ensure a zero value of the determinant of the system (20) defines the critical buckling stress. From this condition, we find two roots for the critical stress:

$$(\sigma_1-\sigma_f)(\sigma_3-\sigma_f)-\sigma_{1\text{-}3}^2=0\Rightarrow$$
$$\Rightarrow(\sigma_f)_{1,2}=\frac{\sigma_1+\sigma_3\pm\sqrt{4\sigma_{1\text{-}3}^2+(\sigma_1-\sigma_3)^2}}{2} \tag{22}$$

The critical buckling stress corresponds to the root with negative sign. Appropriate value of the half wave numbers n in (17) should also be chosen to provide minimum value of found the critical stress.

Note that the root (22) covers a solution for the plate resting on an elastic foundation of constant stiffness ($\Lambda_1 = \Lambda_0 = \Lambda = const$), similar to the one used in (8). In this case, $\Lambda_1^* = \Lambda_3^* = \Lambda$, $\Lambda_{13}^* = 0$, $\sigma_{1\text{-}3} = 0$, and values σ_1, σ_3 define the classical critical buckling stress of the first and third eigenforms of the plate. From (22) it follows then that $(\sigma_f)_{1,2} = (\sigma_1 + \sigma_3 \pm |\sigma_1 - \sigma_3|)/2$ and due to $\sigma_1 < \sigma_3$ we obtain that $(\sigma_f)_1 = \sigma_3$ and $(\sigma_f)_2 = \sigma_1$.

Finite element validation of the solution (22) was obtained using Ansys, for a plate made of three sections of different stiffnesses of the elastic foundation (*elastic support* settings in Ansys). Finite element mesh is shown in Fig. 7a. Comparison between the analytical and numerical solutions is shown in Fig. 7b. It is seen that, for different ratios Λ_1/Λ_0, b/d and α solutions coincide.

References

Aimmanee, S., & Vinson, J. R. (2002). Analysis and optimization of foam-Reinforced web core composite sandwich panels under in-Plane compressive loads. *Journal of Sandwich Structures and Materials, 4*(April), 115–139. doi:10.1106/109963602021030.

Bapanapalli, S. K., Martinez, O. M., Gogu, C., Sankar, B. V., Haftka, R. T., & Blosser, M. L. (2006). Analysis and design of corrugated core sandwich panels for thermal protection systems of space vehicles. In *AIAA paper 1942* (pp. 1–18).

Bin, H., Bo, Y., Yu, X., Chang-Qing, C., Qian-Cheng, Z., & Tian Jian, L. (2015). Foam filling radically enhances transverse shear response of corrugated sandwich plates. *Materials and Design, 77*, 132–141. doi:10.1016/j.matdes.2015.03.050.

Birman, V., & Kardomatea, G. A. (2018). Review of current trends in research and applications of sandwich structures. *Composites Part B: Engineering, 142*, 221–240.

Bitzer, T. (2012). *Honeycomb technology: Materials, design, manufacturing, applications and testing*. Springer Science & Business Media.

Briscoe, C. R., Mantell, S. C., & Davidson, J. H. (2010). Shear buckling in foam-filled web core sandwich panels using a Pasternak foundation model. *Thin-Walled Structures, 48*(6), 460–468. doi:10.1016/j.tws.2009.12.005.

Briscoe, C. R., Mantell, S. C., Davidson, J. H., & Okazaki, T. (2011). Design procedure for web core sandwich panels for residential roofs. *Journal of Sandwich Structures and Materials, 13*(1), 23–58. doi:10.1177/1099636210365441.

Buznik, V., Lurie, S. A., Solyaev, Y. O., Dudchenko, A., Volkov-Bogorodsky, D. B., & Koshurina, A. (2016). Designing a multilayer panel with heat-insulating filler and heat-shielding external coating. *Composites: Mechanics, Computations, Applications: An International Journal, 7*(2), 135–159.

Han, B., Qin, K. K., Yu, B., Zhang, Q. C., Chen, C. Q., & Lu, T. J. (2015). Design optimization of foam-reinforced corrugated sandwich beams. *Composite Structures, 130*, 51–62. doi:10.1016/j.compstruct.2015.04.022.

Kerr, B. A. D. (1985). On the determination of foundation model parameters. *Journal of Geotechnical Engineering, 111*(11), 1334–1340. doi:10.1061/(ASCE)0733-9410(1985)111:11(1334).

Lu, T., Valdevit, L., & Evans, A. (2005). Active cooling by metallic sandwich structures with periodic cores. *Progress in Materials Science, 50*(7), 789–815.

Lurie, S., Solyaev, Y., Volkov-Bogorodskiy, D., Bouznik, V., & Koshurina, A. (2017). Design of the corrugated-core sandwich panel for the arctic rescue vehicle. *Composite Structures, 160*. doi:10.1016/j.compstruct.2016.10.123.

Lurie, S., Solyaev, Y. O., Koshurina, A., Formalev, V., Dobryanskiy, V., & Kachanov, M. (2018). Design of the corrugated-core sandwich panel with external active cooling system. *Composite Structures, 188*, 278–286.

Martinez, O. A., Sankar, B. V., Haftka, R., Bapanapalli, S. K., & Blosser, M. L. (2007). Micromechanical analysis of composite corrugated-core sandwich panels for integral thermal protection systems. *AIAA Journal, 45*(9), 2323–2336.

Njuguna, J. (2016). *Lightweight composite structures in transport: design, manufacturing, analysis and performance*. Woodhead publishing.

Timoshenko, S. P., & Gere, J. M. (1961). *Theory of elastic stability*. McGraw Hill..

Vasiliev, V. V., & Morozov, E. V. (2013). *Advanced mechanics of composite materials and structural elements*. Newnes.

Vescovini, R., D'Ottavio, M., Dozio, L., & Polit, O. (2018). Buckling and wrinkling of anisotropic sandwich plates. *International Journal of Engineering Science, 130*, 136–156.

Vinson, J. (1999). *The behavior of sandwich structures of isotropic and composite materials*. New York: Routledge.

Vinson, J. R. (2005). Sandwich structures: Past, present, and future. In *Sandwich structures 7: Advancing with sandwich structures and materials* (pp. 3–12). Springer.

Wang, L., Liu, W., Wan, L., Fang, H., & Hui, D. (2014). Mechanical performance of foam-filled lattice composite panels in four-point bending: Experimental investigation and analytical modeling. *Composites Part B: Engineering, 67*, 270–279. doi:10.1016/j.compositesb.2014.07.003.

Xie, G., Wang, C., Ji, T., & Sunden, B. (2016). Investigation on thermal and thermomechanical performances of actively cooled corrugated sandwich structures. *Applied Thermal Engineering, 103*, 660–669.

Yu, L. H., & Wang, C. Y. (2008). Buckling of rectangular plates on an elastic foundation using the levy method. *AIAA Journal, 46*(12), 3163–3167. doi:10.2514/1.37166.